

Lithographically Defined Three-Dimensional Graphene Scaffolds

D. Bruce Burkel^{a*}, Xiaoyin Xiao^a, and Ronen Polsky^a

^a Sandia National Laboratories, P.O. Box 5800, Albuquerque New Mexico, 87185

ABSTRACT

Interferometrically defined 3D photoresist scaffolds are formed through a series of three successive two-beam interference exposures, a post exposure bake and development. Heating the resist scaffold in a reducing atmosphere to $> 1000^{\circ}\text{C}$, results in the conversion of the resist structure into a carbon scaffold through pyrolysis, resulting in a 3D sp_3 -bonded glassy carbon scaffold which maintains the same in-plane morphology as the resist despite significant shrinkage. The carbon scaffolds are readily modified using a variety of deposition methods such as electrochemical, sputtering and CVD/ALD. Remarkably, sputtering metal into scaffolds with ~ 5 unit cells tall results in conformal coating of the scaffold with the metal. When the metal is a transition metal such as nickel, the scaffold can be re-annealed, during which time the carbon diffuses through the nickel, emerging on the exterior of the nickel as sp_2 -bonded carbon, termed 3D graphene. This paper details the fabrication, characterization and some potential applications for these structures.

Keywords: 3D carbon, lithography, pyrolysis

1. INTRODUCTION

Since the exfoliation method for synthesis of single layer graphene was discovered¹, interest and research into graphene and application of graphene to a wide variety of technology needs has expanded dramatically. Graphene has been used in applications from touch screens, fuel cells, electronics and materials all owing to the exotic material properties afforded by the sp_2 bonds forming the in-plane bonding of the graphene sheet. Given the interest in application of graphene, pursuit of more manufacturable and scalable methods for creating high quality graphene has emerged as a new thrust in the research community^{2,3}. Recently several research groups have undertaken the synthesis of 3D graphene. Johnson et. al. used carbon occurring in wood, along with the celluloid structure to create 3D porous graphitic carbon⁴. Yufeng et. al. used a hydrogel self-assembly process to create porous graphitic material at low temperatures and atmospheric pressure⁵.

It is well known that chemical vapor deposition of carbon on transition metals such as copper and nickel chemically templates the carbon formation into sp_2 -bonded graphene⁶. Several groups have taken advantage of this effect to produce 3D graphene^{7,8}. Starting from nickel foam, a three-dimensional scaffold of electroformed nickel with pores ~ 100 s of micrometers in diameter, carbon is conformally deposited via chemical vapor deposition (CVD), coating the nickel scaffold, which chemically templates the carbon into sp_2 bonds, forming a 3D graphitic carbon scaffold termed 3D graphene. The nickel can then be etched out using an acidic etchant, leaving a hollow 3D network of graphene. The sp_2 bonds form a planar sheet. In allotropes such as carbon nanotubes, these sheets can be rolled into self-terminating tubes for orientations with perfect winding numbers. For 3D carbon, it is not possible to achieve perfect winding numbers in all three dimensions simultaneously, so the graphene forming the scaffold buckles, appearing as faceted patches with edges and dislocations to accommodate the formation of the 3D scaffold with an inherently 2D sheet. Even though the graphene sheets buckle and generate significant edge dislocations and imperfections, the quality of the graphene is quite high as measured by x-ray photoelectron spectroscopy (XPS) and micro-Raman spectroscopy. In all of these synthesis methods, the pore size distribution is stochastically determined by some thermodynamically governed process.

Recently, we have demonstrated conversion of lithographically created 3D structures with controlled pore size and scaffold morphology in photoresist into scaffolds of sp_3 bonded carbon through pyrolysis⁹⁻¹⁴. These structures are mechanically robust, have nearly DC metallic conductivity. Because they are essentially glassy carbon, the material of choice for as the standard carbon electrode (SCE) they are readily electrochemically modified through deposition of nanoparticles and electro-conductive polymers^{15,16}. These structures can also be modified via physical vapor deposition,

*dbburck@sandia.gov

by sputtering into the carbon matrix. We have shown that PVD of Ag films results in conformal coverage of the scaffolding¹⁷. Here we report on the conversion of these 3D sp₃ bonded carbon scaffolds into 3D sp₂ bonded scaffolds through a modified version of the conversion process used to create 3D carbon via the nickel foam approach.

2. SCAFFOLD FORMATION

We use interferometric lithography (IL) to form 3D patterns in thick photoresist. In IL, coherent plane waves are interfered in space, generating a 2D fringe pattern. When an ultraviolet laser is used, the fringe pattern can be used to expose photoresist. For this work, a tripled frequency Nd:YAG laser (355 nm) was used so that commercially available i-Line photoresists can be exposed. Both novolac resin (NR-7 Futurrex) as well as photoepoxy (SU-8, microchem) can be used. In the case of negative photoresist, the resist is a non-linear medium, accumulating exposure dose, forming chemically amplified bonds in the interior of the resist. The result is that multiple exposures with intermediate rotations of the substrate between exposures results in the creation of a latent 3D image in the volume of the photoresist¹⁸. One particularly attractive property of SU-8 is its transparency and small index change after cross-linking, allowing exposures in extremely thick resist stacks.

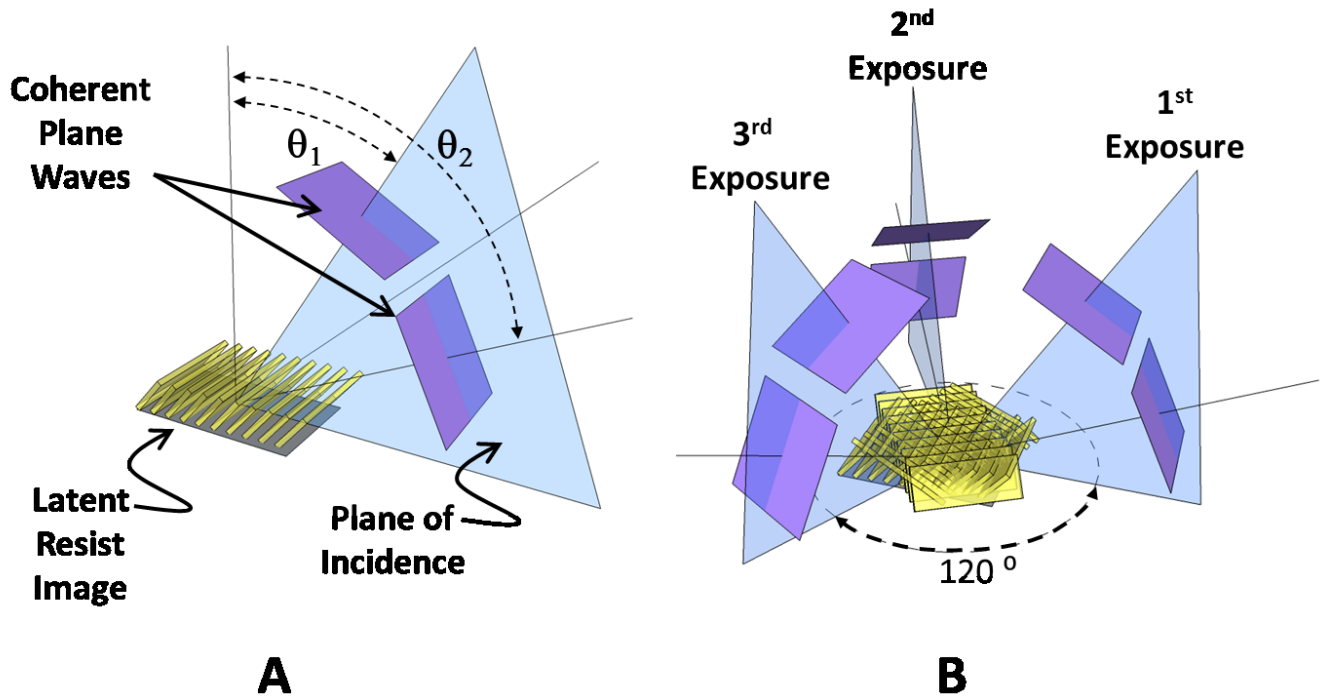


Fig. 1 A.) Schematic diagram of a tilted two-beam interferometric exposure; B.) Schematic diagram of three two-beam exposures with rotation in order to create a three dimensional resist scaffold.

Depending on the number of exposures and the relative rotations between them, after development, 1D, 2D and 3D photoresist pattern can result. For a single exposure with the beams symmetrically disposed about the surface normal, 1D line patterns are formed in the resist. For a single exposure with the beams assymmetrically disposed about the surface normal, tilted lines are formed in the resist. By rotating the sample in plane, a second exposure can be performed prior to post-exposure bake, creating periodicity in a second direction. For rotations of 90 degrees, the result is a square lattice of holes. For a rotation of 60 degrees, the pattern is a triangular lattice of elliptical holes. For 3 successive 2-beam exposures tilted with respect to the substrate normal with 120 degrees of rotation of the substrate between the exposures the result is a nearly face-centered-cubic 3D lattice. Due to the index mismatch between the resist film and air, it is not possible to expose the resist stack at a steep enough angle to achieve an exact FCC geometry. After all the cumulative exposures, the resist undergoes a post exposure bake, followed by a hard bake. The resist pattern is then heated to >

1000 °C in flowing forming gas (5% H₂, 95% N₂). The non-carbon species in the resist are volatilized and boil off, while the carbon remains behind. There is significant shrinkage of the photoresist pattern, but the basic morphology remains intact. The result is a 3D network of sp₃-bonded carbon with micron-scale porosity.

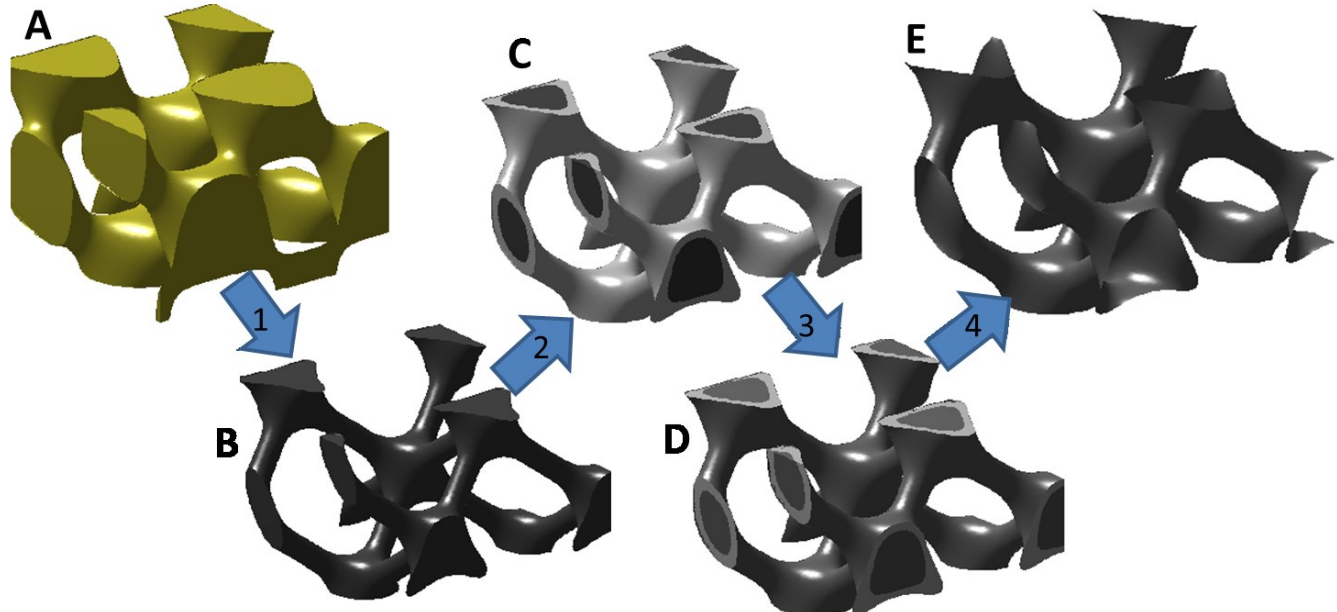


Fig. 2 Starting with a 3-Dimensional resist scaffold (A), perform pyrolysis (step 1) to create an sp₃-bonded carbon structure (B); sputter nickel (step 2) to create a nickel coated carbon scaffold (C); Anneal at high temperature (step 3), diffusing carbon through nickel and templating graphene on the surface (note nickel and carbon trade places during this step); Dissolve out nickel in hydrochloric acid (step 4) to yield a hollow 3D graphene matrix.

3. CONVERSION TO GRAPHENE

Whereas the generic prescription for the formation of 3D graphene starts from a pre-formed 3D nickel scaffold, in order to convert this scaffold into sp₂-bonded carbon, nickel is sputtered into the 3D carbon scaffold. As with the Ag films used for Raman sensing, this sputtering results in conformal coverage of the carbon scaffold. After a subsequent anneal, the carbon diffuses through the nickel coating. In a rather remarkable turn of events, the nickel and carbon completely switch places, forming a hollow, 3D scaffold of nickel-carbon. The conversion of the carbon into an sp₂-bonded carbon can be confirmed via x-ray spectroscopy. Since XPS is a surface technique, with penetration depth < 1nm, it is apparent that the nickel and carbon have completely switched places¹⁹⁻²¹.

Micro-Raman scanning is another technique which can be used to assess both the quality of the graphene as well as the number of graphene layers present. In micro-Raman scanning, an incident laser is focused down with the scattered light collected by an objective, such that a spatial map of a surface with resolution of ~ can be acquired. By fitting the center peaks of the Raman active modes as well as fitting the peak shape, detailed analysis of the degree of sp₂ to sp₃-bonding and the number of layers can be discerned. Using this approach, we are able to determine that our scaffolds are converted to sp₂-bonded carbon with regions of material with both < 5 layers and > 5 layers of sp₂-bonded carbon.

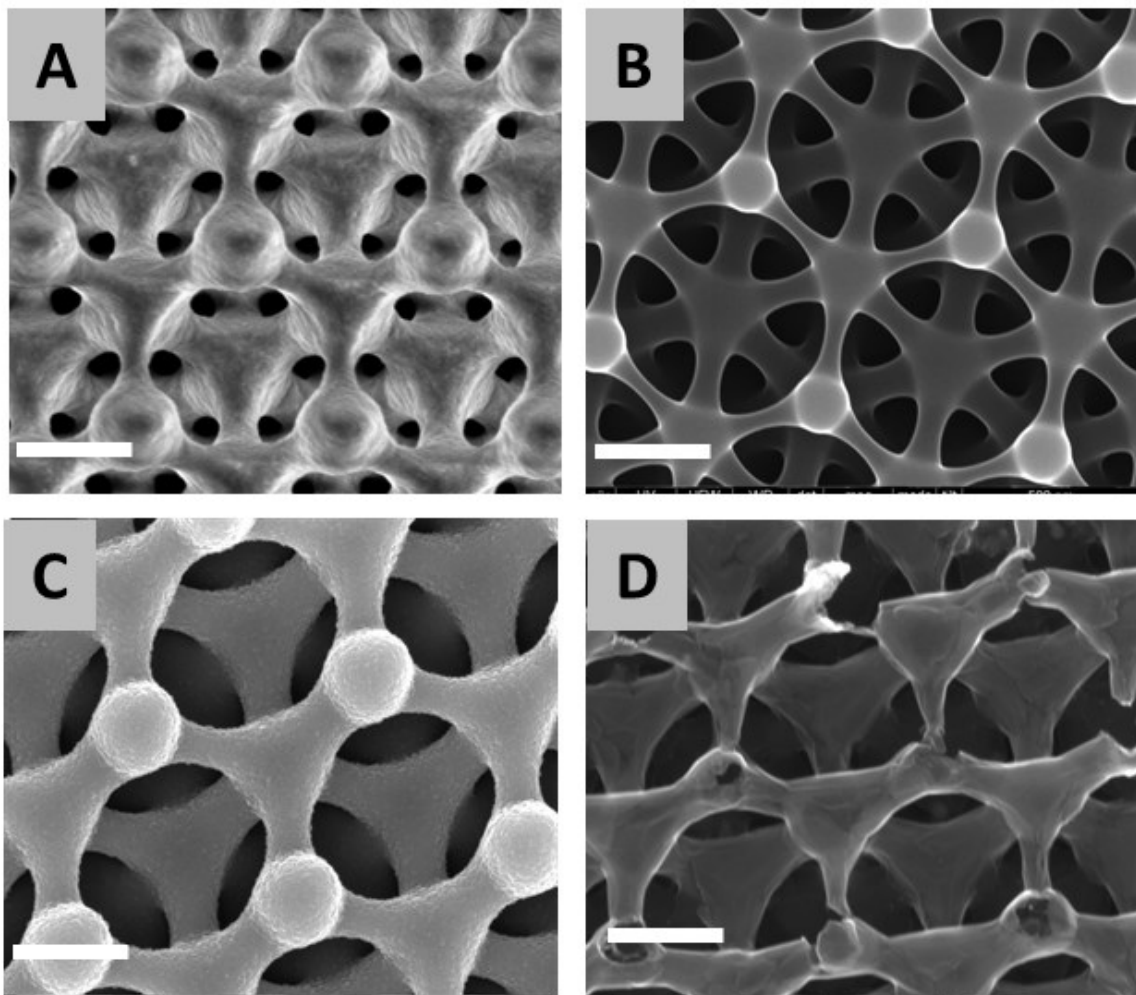


Fig. 3 Top-down scanning electron micrographs of (A) Three-dimensional resist scaffold; (B) Pyrolyzed sp₃-bonded carbon scaffold; (C) Conformal nickel-coated sp₃-bonded carbon scaffold (pre-anneal); (D) Three-dimensional sp₂-bonded (3D Graphene) scaffold. The scale bars are 500 nm.

4. APPLICATIONS

Having converted the carbon from sp₃-bonded carbon to sp₂-bonded carbon has distinct advantages for electrochemical sensing applications. For instance, dopamine, uric acid and ascorbic acid can all be present in biological specimens. All three substances possess similar oxidation potential windows versus glassy carbon electrodes, making simultaneous detection difficult. We have shown that 3D graphene possesses a catalytic activity toward ascorbic acid oxidation, separating the oxidation peaks and allowing for simultaneous detection of all three substances in a single solution without any further modification of the electrode²².

ACKNOWLEDGEMENTS

Supported by the Laboratory Directed Research and Development program at Sandia National Laboratories, a multi-program laboratory managed and operated by Sandia Corporation, a wholly owned subsidiary of Lockheed Martin Corporation, for the U.S. Department of Energy's National Nuclear Security Administration under contract DE-AC04-94AL85000.

REFERENCES

- [1] Novoselov, K. S. , Geim, A. K. , Morozov, S. V. , Jiang, D. , Zhang, Y. , Dubonos, S. V. , Grigorieva, L. V. , Firsov, A. A. , "Electric field effect in atomically thin carbon films," *Science*, **306**, 666-669 (2004).
- [2] Sun, Z., Yan, Z., Yao, J., Beitler, E, Zhu, Y., and Toure, J.M., "Growth of graphene from solid carbon sources," *Nature*, **468**, 549-552 (2010).
- [3] Ruan, G., Sun, Z., Peng, Z. and Toure, J.M., "Growth of graphene from food, insects and waste," *ACS Nano*, **5**, 7601-7607, (2011).
- [4] Johnson, M. T. and Faber, K. T. , "Catalytic graphitization of three-dimensional wood-derived porous carbon scaffolds," *J. Mat Research*, **26**, 18-25 (2011).
- [5] Chen, W. and Yan, L., "In situ self-assembly of mild chemical reduction graphene for three-dimensional architectures," *Nanoscale*, **3**, 3132-3137, (2011).
- [6] Peng, Z., Yan, Z., Sun, Z. and Toure, J. M., "Direct growth of bilayer graphene on SiO₂ substrates by carbon diffusion through nickel," *ACS Nano*, **5**, 8241-8247 (2011)
- [7] Chen, Z., Ren, W., Gao, L., Liu, B., Pei, S., and Cheng, H.M., "Three-dimensional flexible and conductive interconnected graphene networks grown by chemical vapor deposition," *Nat. Mater.*, **10**, 424-428 (2011).
- [8] Cao, X., Shi, Y., Shi, W., Lu, G., Huang, X., Yan, Q., Zhang, Q., and Zhang, H., "Preparation of novel 3D graphene networks for supercapacitor applications," *Small*, **7**, 3163-3168 (2011).
- [9] Burckel, D. B., Fan, H. Y., Thaler, G., and Koleske, D. D., "Lithographically defined carbon growth templates for ELOG of GaN," *J. of Cryst. Growth*, **310**, 3113-3116 (2008).
- [10] Burckel, D. B., Washburn, C. M., Raub, A. K., Brueck, S. R. J., Brozik, S. M., Wheeler, D. R. and Polksky, R., "Lithographically defined porous carbon electrodes," *Small*, **5** (24), 2792-2796 (2009).
- [11] McCreery, R. L., "Advanced carbon electrode materials for molecular electrochemistry" *Chem. Rev.* **108**, 2646-2687 (2008).
- [12] Lyons, A. M., "Photodefinable carbon films: Electrical properties" *J. Non-Cryst. Solids* **70**, 99-109 (1985).
- [13] Schueller, O. J. A. , Brittain, S. T. and Whitesides, G. M. , "Fabrication of glassy carbon microstructures by pyrolysis of microfabricated polymeric precursors," *Adv. Mater.* **9**, 477-480 (1997).
- [14] Ranganathan, S. , McCreery, R. , Majii, S. M. and Madou, M. J., J. "Photoresist-derived carbon for microelectromechanical systems and electrochemical applications," *J. of Electrochem. Soc.* **147**, 277-282 (2000).
- [15] Sattayasamitsathit, S., O'Mahony, A. M., Xiao, X., Brozik, S. M., Washburn, C. M., Wheeler, D. R., Cha, J., Burckel, D. B., Polksky R., and Wang, J., "Highly dispersed Pt nanoparticle-modified 3D porous carbon: A metallized carbon electrode material," *Electrochem. Comm.*, **13** (8), 856-860, (2011).

[16] Xiao, X., Roberts, M. E., Wheeler, D. R., Washburn, C. M., Edwards, T. L., Brozik, S. M., Montano, G. A., Bunker, B. C., Burckel, D. B., and Polsky, R., "Increased mass transport at lithographically defined 3-D porous carbon electrodes," *ACS Appl. Mater. And Inter.*, **2** (11), 3179-3184 (2010).

[17] Xiao, X., Nogan, J., Beechem, T. E., Montano, G. A., Washburn, C. M., Wang, J., Brozik, S. M., Wheeler, D. R., Burckel, D. B., and Polsky, R., "Lithographically-defined 3D porous networks as active substrates for surface enhanced Raman scattering," *Chem. Comm.*, **47** (35), 9858-9860 (2011).

[18] Burckel, D. B., Washburn, C. M., Koleske, D. D., and Polsky, R., "Pyrolysis of two-dimensional and three-dimensional interferometrically patterned resist structures," *J. of Vac. Sci. and Tech. B*, **28** (6), C6P14-C6P17 (2010).

[19] Xiao, X., Beechem, T.E., Brumbach, M. T., Lambert, T. N., Davis, D. J., Michael, J. R., Washburn, C. M., Wang, J., Brozik, S. M., Wheeler, D. R., Burckel, D. B. and Polsky, R., "Lithographically defined three-dimensional graphene structures," *ACS Nano*, **6** (4), 3573-3579 (2012).

[20] Xiao, X., Michael, J. R., Beechem, T.E., McDonald,A., Rodriguez, M., Brumbach, M. T., Lambert, T. N., Washburn, C. M., Wang, J., Brozik, S. M., Wheeler, D. R., Burckel, D. B., and Polsky, R., "Three-dimensional nickel-graphene core-shell electrodes," *J. of Mat. Chem.*, **22**, 23749-23754 (2012).

[21] Sattayasamitsathit, S., Gu, Y., Kaufmann, K., Jia, W., Xiao, X., Rodriguez, M., Minteer, S., Cha, J., Burckel, D. B., Wang, C., Polsky R., and Wang, J., "Highly ordered multilayered 3D graphene decorated with metal nanoparticles," *J. of Mat. Chem. A*, **1**, 1639-1645 (2013).

[22] Xiao, X., Miller, P. R., Narayan, R. J., Brozik, S. M., Wheeler, D. R., Brener, I., Wang, J., Burckel, D. B., and Polsky, R., "Simultaneous detection of dopamine, ascorbic acid and uric acid at lithographically-defined 3D electrodes," *Electroanal.*, **26**, 52-56 (2014).